

Supplementary Information

Flexible-in-rigid polycrystalline titanium nanofibers: A toughen strategy from macro-scale to molecular-scale

Wanlin Fu^{1†}, Wanlin Xu^{1†}, Kuibo Yin^{2†}, Xiangyu Meng¹, Yujie Wen³, Luming Peng³, Mingyu Tang¹, Litao Sun², Yueming Sun¹ & Yunqian Dai^{1*}

¹School of Chemistry and Chemical Engineering, Southeast University, Nanjing, Jiangsu 211189, P. R. China

²SEU-FEI Nano-Pico Center, Key Laboratory of MEMS of Ministry of Education, School of Electronic Science and Engineering, Southeast University, Nanjing, Jiangsu 211189, P. R. China

³Key Laboratory of Mesoscopic Chemistry of Ministry of Education, School of Chemistry and Chemical Engineering, Nanjing University, Nanjing, 210023, China

*Address corresponding to: daiy@seu.edu.cn

†These three authors contributed equally to this work.

Experimental section

Materials

Polyvinylpyrrolidone (PVP), titanium isopropoxide (TTIP) and aluminum acetylacetonate ($\text{Al}(\text{acac})_3$) were obtained from Alfa Aesar. All chemicals were used as received. The water used in all experiments was filtered through a Millipore filtration system with a resistivity of $18 \text{ M}\Omega \cdot \text{cm}$.

Fabrication of flexible-in-rigid TiO_2 -based nanofibers

The TiO_2 -based nanofibers were prepared by electrospinning a precursor containing 0.6 g of PVP ($M_w \approx 1.3 \times 10^6$), 4.5 mL of ethanol, a certain amount of $\text{Al}(\text{acac})_3$, 5 mL of acetone, 2.5 mL of TTIP and 3 mL of acetic acid with a flow rate of 0.3 mL/h, at 18 kV followed by calcination at $900 \text{ }^\circ\text{C}$ for 2 h in air with a ramping rate of $2.8 \text{ }^\circ\text{C}/\text{min}$. The atomic ratio of Al to (Al+Ti) was controlled to be 0 (unmodified TiO_2 nanofibers, named as AT-0), 10% (named as AT-10), 30% (named as AT-30) and 50% (named as AT-50) in resultant nanofibers.

In situ heating experiment

The structural evolution of the TiO_2 -based nanofibers during *in situ* heating was dynamically observed on FEI Titan 80-300 TEM microscope, using an electrical chip (E-chip)-based single-tilt heating holder (Aduro, Protochips Company). The nanofibers were firstly dispersed on a Si_3N_4 E-chip, then loaded in the heating holder and inserted into the microscope chamber. The temperature was precisely controlled from room temperature increased to $700 \text{ }^\circ\text{C}$ in 1 s and stabilized for 10 min, then further elevated to 750, 800, 850, and $900 \text{ }^\circ\text{C}$ with ramping rate of $30 \text{ }^\circ\text{C}/\text{min}$ and hold for 10 min, respectively. Because of the high nominal ramp rate of the heating holder ($1000 \text{ }^\circ\text{C}/\text{ms}$), the temperatures of the nanofibers are assumed to reach the set value immediately after switching on the current. For structure imaging, low beam densities (typically, $60 \text{ A}/\text{cm}^2$) were used to reduce the irradiation-induced sputtering effects.

Mechanical performance measurement

Fibrous mat was carefully cut into rectangular shape with size of $20 \times 5 \text{ mm}$ for each test. The thickness of each sample was controlled to be $\sim 15 \text{ }\mu\text{m}$. The stress-strain tests were conducted on Keysight UTM150 with a tension trigger of $250 \text{ }\mu\text{N}$ and strain rate of $10^{-3}/\text{s}$ at room temperature ($\sim 20 \text{ }^\circ\text{C}$) with humidity of $\sim 40\%$.

Simulations of electric field distribution and stress distribution

The electric field distribution was studied starting from the metal spinneret to the surface of electrospinning receptor, using COMSOL Multiphysics. The inner radius, external radius, and

length of metal spinnerets were set as 0.20 mm, 0.35 mm, and 25 mm, respectively. The distance between the spinneret tip and the surface of electrospinning receptor was set as 12.5 cm. The voltage was set as 18 kV. For three-spinnerets system, the neighboring distance between two spinnerets was set as 0.5 cm. All these parameters were in accordance with the used electrospinning set-up.

The stress distribution was simulated by the Structural Mechanics, Solid Mechanics, Stationary Domain interface in COMSOL Multiphysics. Geometries were built based on SEM observations, BET results, and mechanical tests. All the model nanofibers were set as those with 300 nm in diameter, 1500 nm in height, 4.1 g/cm³ in density, 653.8 MPa in Young's modulus and 0.4 in Poisson's ratio. Fixed Constraint was used at bottom surface of the simulated fiber. Boundary Load was set with a total force of 1000 N/m², with upward direction. For investigating the effect of length-diameter ratio, the length-diameter ratios were set as 5:1 and 25:1 respectively. To reveal the role of pore size on stress distribution, the pore diameters were set as 50 nm and 10 nm respectively. And the numbers of pore within an individual nanofiber were set as 40 and 100 respectively, to study the relationship between pore density and mechanical performance.

Filtration efficiency measurement

The PM filtration performance of the mats was evaluated on an LZC-H filter tester (Huada Filter Technology Co., Ltd., China). Before the filtration test, the fibrous mat (with a thickness of ~15 μm) was clamped by a 10 cm diameter holder. Next, 300,000–500,000 NaCl particles were neutralized charge by electrostatic neutralization device and delivered through the test mat steadily and uniformly. The pressure drop was monitored by two electronic pressure transducers under designed airflow of 32, 64, and 80 L/min. All of the air filtration tests were conducted at ambient temperature (25 ± 2 °C), and humidity (35 ± 5%).

The long-term stability test was carried out in a home-made setup. The fibrous mats and sponges were placed on a circular hole with a diameter of 1 cm above the box, and the number of particles was measured every 20 minutes. The filtration efficiency η was evaluated by equation (1):

$$\eta = \frac{N_0 - N_1}{N_0} \times 100\% \quad (1)$$

where η is the filtration efficiency, N_0 , N_1 are correspond to the number of PM particles inside the box and outside the AT mat.

The quality factor (QF) is defined as:

$$QF = [-\ln (1-\eta)]/\Delta p \quad (2)$$

where η and Δp represent the filtration efficiency and pressure drop, respectively.

Characterizations

Scanning electron microscopy (SEM) images were obtained using FEI microscope (Inspect F50). Transmission electron microscope (TEM) images were collected using Tecnai G2 T20, FEI operated at 200 kV. Energy dispersive X-ray (EDX) mapping and HAADF-STEM analysis were performed using Talos. The crystal structure information was obtained with X-ray diffraction (Bruker, D8 advance using Cu-K α radiation, $\lambda=1.5406 \text{ \AA}$). Brunner–Emmet–Teller (BET) surface area was tested by Nova 1200e (Quantachrome, USA). High resolution Raman spectrum were collected by Acton SpectraPro SP-2300 (Princeton instruments) with a 532 nm laser. X-ray photoelectron spectroscopy (XPS) measurements were carried out on an ESCALAB 250Xi spectrometer (Thermo Scientific, USA) with a mono-chromatized Al K α X-ray source. Solid-state NMR experiments were performed using a Bruker Avance III spectrometer.

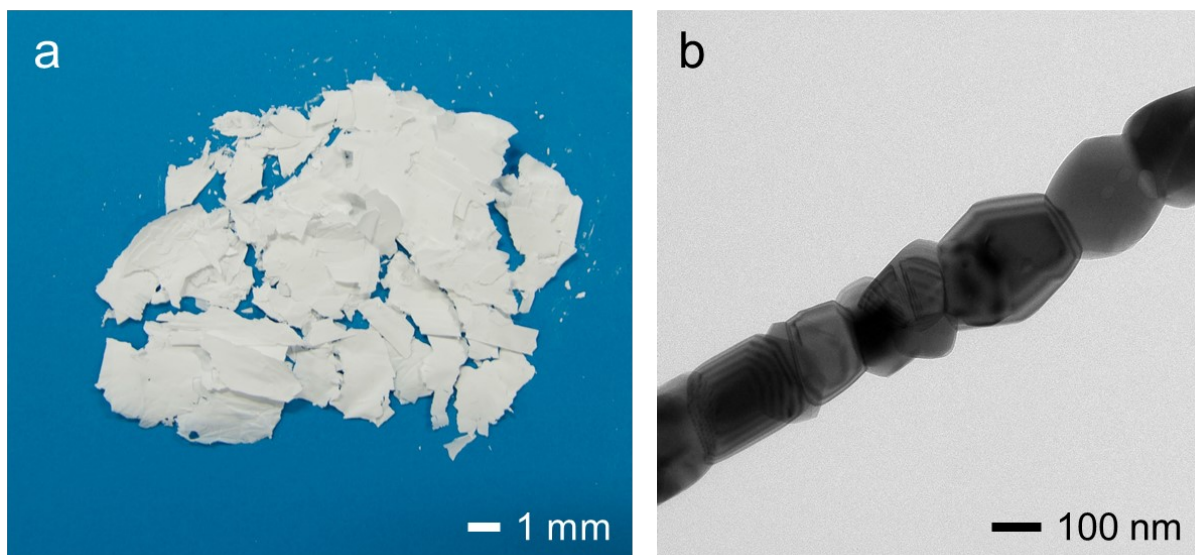


Fig. S1 Pristine brittle TiO_2 nanofibers. (a) Optical image of the TiO_2 debris. (b) TEM image of one TiO_2 nanofiber calcined at $900\text{ }^\circ\text{C}$.

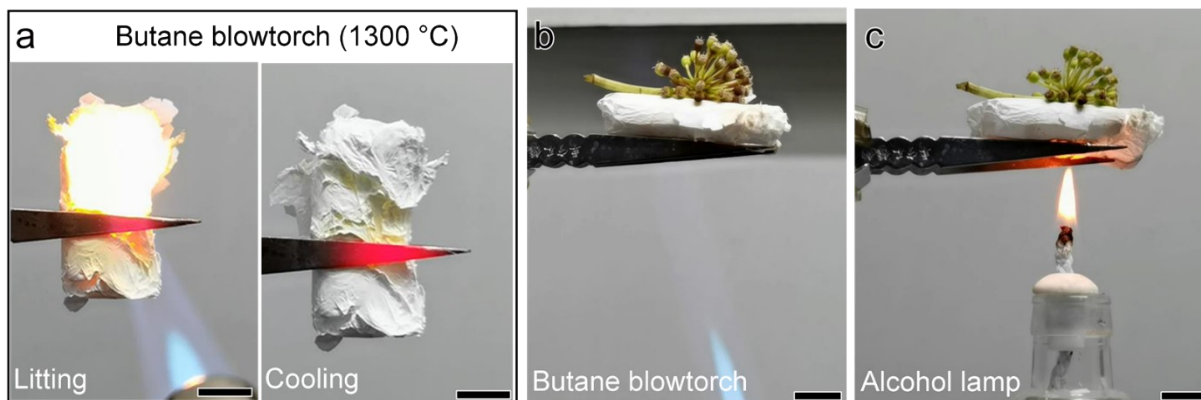


Fig. S2 High-temperature resistance and flammability. (a) Optical images of a AT-30 sponge treated by butane blowtorch. (b–c) Illustration of superior thermal insulation performance of a AT-30 sponge.

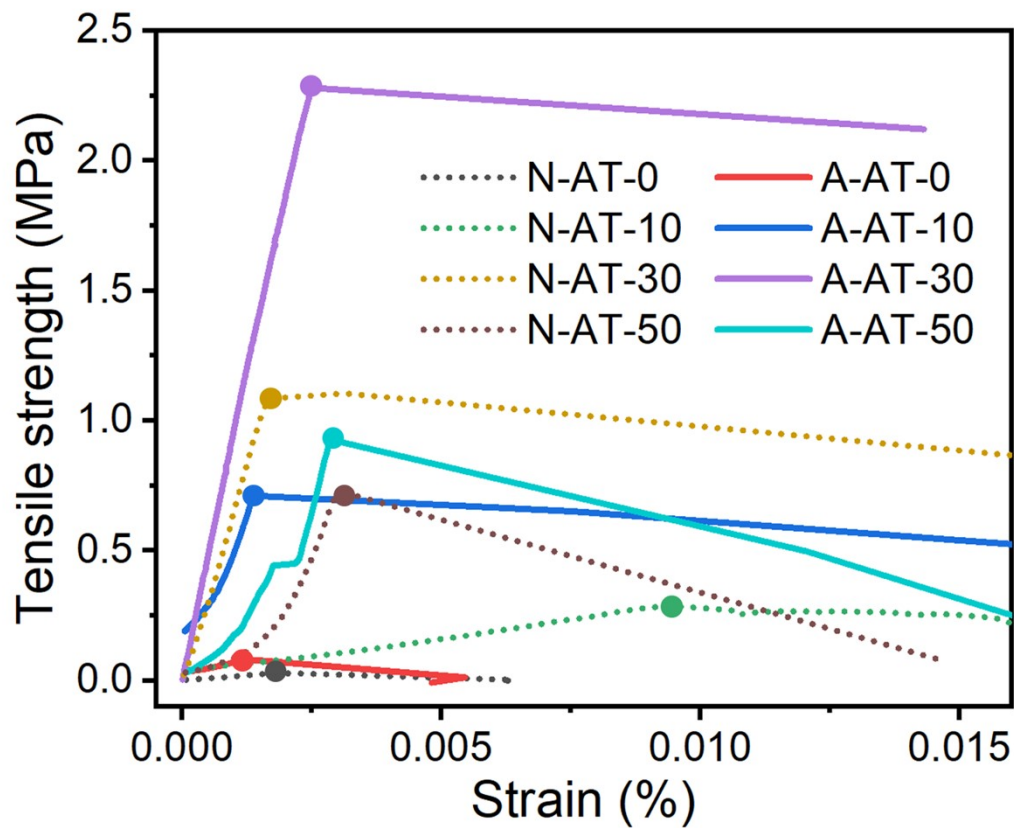


Fig. S3 Tensile stress-strain curves of AT-*n* fibrous mats.

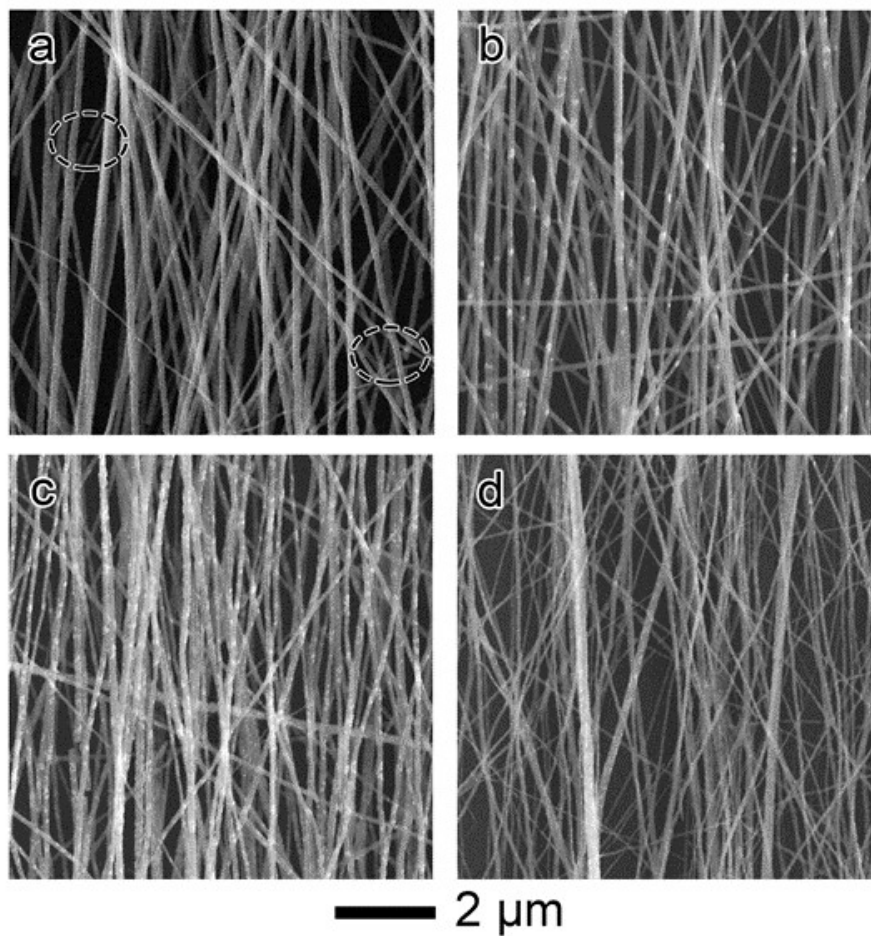


Fig. S4 SEM images of aligned AT-0, AT-10, AT-30, and AT-50 mats. The dashed circles highlight the crack of unmodified TiO₂ nanofibers.

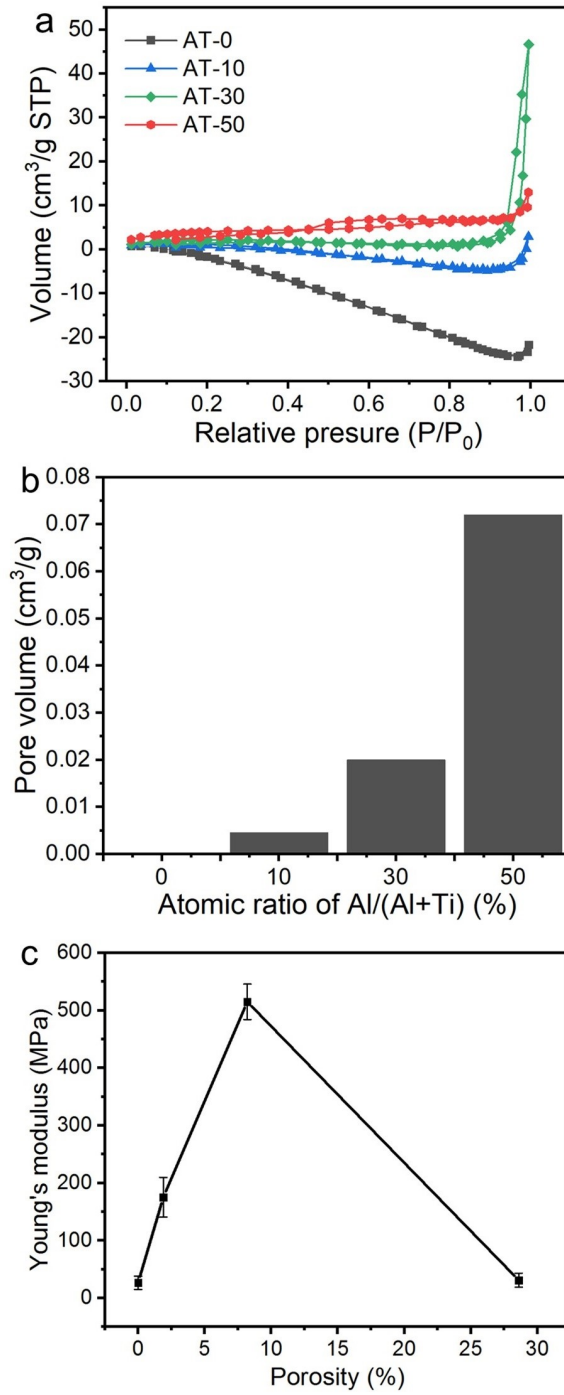


Fig. S5 (a) The nitrogen physisorption isotherms and (b) pore volume distributions of the AT-*n* nanofibers. (c) The Young's modulus *versus* porosity.

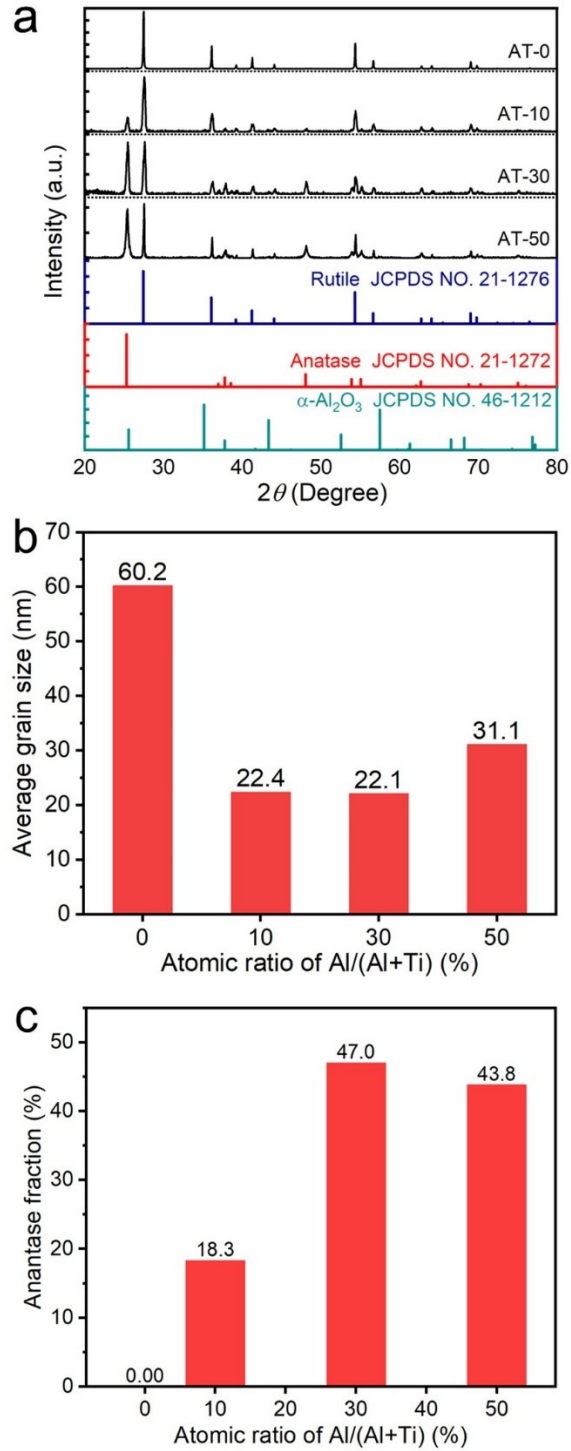


Fig. S6 (a) XRD patterns, (b) the corresponding crystal sizes and (c) the calculated anatase fraction of AT-0, AT-10, AT-30 and AT-50 nanofibers calcined at 900 °C.

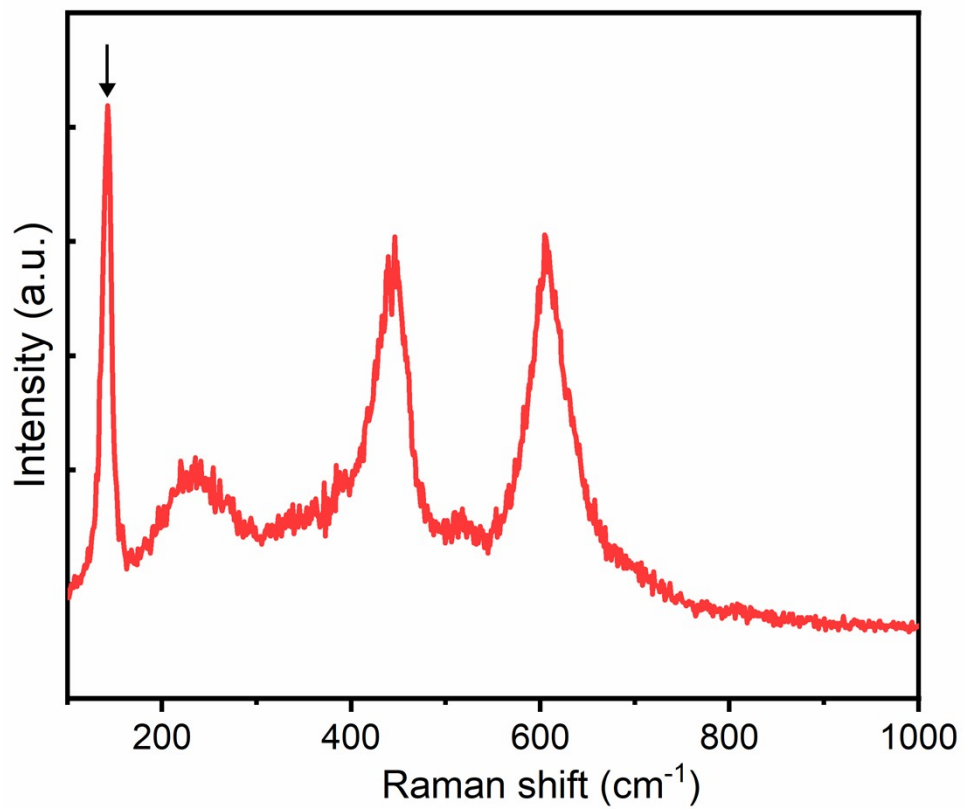


Fig. S7 Raman spectra of-AT-30 nanofibers.

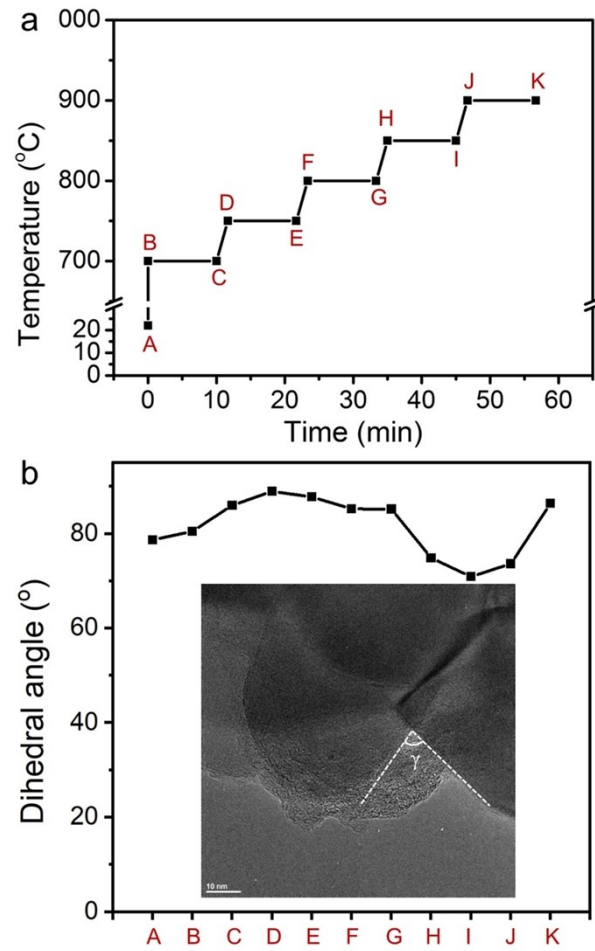


Fig. S8 (a) *In situ* heating temperature profile. (b) Evolution of dihedral angle (γ) between two neighboring TiO_2 grains during heat-treatment.

Supplementary Movies

Supplementary Video S1. Expansion and folding of the fibrous mat.

Supplementary Video S2. Elastic display of the fibrous sponge.

Supplementary Video S3. The fibrous sponge heated by the butane blowtorch for 60 s.

Supplementary Video S4. Heat resistance display of the fibrous sponge.

Supplementary Video S5. *In-situ* heating observation of unmodified TiO₂ nanofibers by TEM.